A 10-Approximation of the $\frac{\pi}{2}$-MST

Ahmad Biniaz ✉
School of Computer Science, University of Windsor, Canada

Majid Daliri ✉
School of Electrical and Computer Engineering, University of Tehran, Iran

Amir Hossein Moradpour ✉
School of Electrical and Computer Engineering, University of Tehran, Iran

Abstract

Bounded-angle spanning trees of points in the plane have received considerable attention in the context of wireless networks with directional antennas. For a point set P in the plane and an angle α, an α-spanning tree (α-ST) is a spanning tree of the complete Euclidean graph on P with the property that all edges incident to each point $p \in P$ lie in a wedge of angle α centered at p. The α-minimum spanning tree (α-MST) problem asks for an α-ST of minimum total edge length. The seminal work of Anscher and Katz (ICALP 2014) shows the NP-hardness of the α-MST problem for $\alpha = \frac{2\pi}{3}, \pi$ and presents approximation algorithms for $\alpha = \frac{\pi}{2}, \frac{2\pi}{3}, \pi$.

In this paper we study the α-MST problem for $\alpha = \frac{\pi}{2}$ which is also known to be NP-hard. We present a 10-approximation algorithm for this problem. This improves the previous best known approximation ratio of 16.

2012 ACM Subject Classification Theory of computation → Computational geometry; Theory of computation → Approximation algorithms analysis

Keywords and phrases Euclidean spanning trees, approximation algorithms, bounded-angle visibility

Digital Object Identifier 10.4230/LIPIcs.STACS.2022.13

Funding *Ahmad Biniaz*: supported by NSERC.

1 Introduction

Wireless antennas in a wireless network can be modeled by disks in the plane, where the centers of the disks represent locations of antennas and their radii represent transmission ranges of antennas. Two antennas can communicate if they are in each other's transmission range. In this model antennas are assumed to be omni-directional which can transmit and receive signals in 360 degrees. Replacing omni-directional antennas with *directional antennas* has received considerable attention in recent years, see for example [1, 3, 6, 8, 9, 10, 11, 13, 14, 21]. Directional antennas can transmit and receive signals only in a circular wedge with some bounded-angle α. As noted in [4, 21, 23] such a bounded-angle communication is more secure, requires lower transmission range, and causes less interference. In this model two antennas can communicate if each one is inside the other's wedge. This model is known as *symmetric communication network* [4, 5, 23].

The network connectivity is a common problem in designing networks with directional antennas. Aschner and Katz [3] formulated this problem in terms of an *α-spanning tree* (α-ST). For a point set P in the plane and an angle α, an α-ST of P is a spanning tree of the complete Euclidean graph on P such that all edges incident to each point $p \in P$ lie in a wedge of angle α centered at p (see Figure 1). It is known that an α-ST always exists when $\alpha \geqslant \frac{\pi}{3}$ (see e.g. [1, 2, 11]) while it may not exists when $\alpha < \frac{\pi}{3}$, for example if P consists of the three vertices of an equilateral triangle.

39th International Symposium on Theoretical Aspects of Computer Science (STACS 2022).
Editors: Petra Berenbrink and Benjamin Monmege; Article No. 13; pp. 13:1–13:15
Leibniz International Proceedings in Informatics
Schloss Dagstuhl – Leibniz-Zentrum für Informatik, Dagstuhl Publishing, Germany

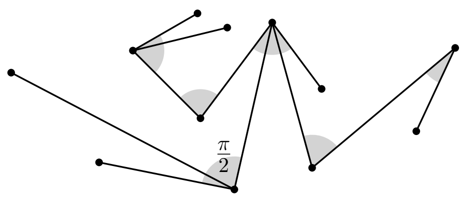

Figure 1 A $\frac{\pi}{2}$-spanning tree.

The minimum spanning tree (MST) is the shortest connected network for omni-directional antennas. For directional antennas, the shortest connected network is called the *α-minimum spanning tree* (α-MST) which is an α-ST of P with minimum total edge length. Although one can compute an MST of n points in the plane optimally in $O(n \log n)$ time, it is not clear how to efficiently compute an α-MST. Aschner and Katz [3] proved that the α-MST problem is NP-hard for $\alpha = \frac{2\pi}{3}$ and $\alpha = \pi$. They also presented approximation algorithms with ratios 16, 6, and 2 for angles $\alpha = \frac{\pi}{2}$, $\alpha = \frac{2\pi}{3}$ and $\alpha = \pi$, respectively. The approximation ratio 6 for the $\frac{2\pi}{3}$-MST has been successively improved to 5.34 [8] and to 4 [6]. Recently Tran et al. [23] showed that the power assignment problem with directional antennas (described in Section 1.2) of angle $\frac{\pi}{2}$ is NP-hard, by a reduction from the Hamilton path problem on hexagonal grid graphs. A similar reduction can be employed to show that the $\frac{\pi}{2}$-MST problem is also NP-hard.

The above approximation ratios are obtained by considering the weight of the MST as the lower bound (instead of the weight of an optimal α-MST). Of these approximation ratios, the ratio 16 for $\frac{\pi}{2}$ is very interesting because for any $\alpha < \frac{\pi}{2}$ there exists a point set for which the ratio of the weight of any α-MST to the weight of any MST is $\Omega(n)$ [5]. In other words, $\alpha = \frac{\pi}{2}$ is the smallest angle for which one can obtain an α-ST of weight within some constant factor of the MST weight. However, such a factor cannot be better than 2 because for points uniformly distributed on a line the weight of α-MST could be arbitrary close to 2 times the weight of MST, for any $\alpha < \pi$ [3, 8].

1.1 Our contributions

We present an algorithm that finds a $\frac{\pi}{2}$-ST of weight at most 10 times the MST weight (Theorem 6). Thus we obtain a 10-approximation algorithm for the $\frac{\pi}{2}$-MST problem, improving upon the previous best known ratio of 16 due to Anscher and Katz [3]. Both our algorithm and that of [3] take linear time after computing an MST.

Towards obtaining the approximation ratio 10 we extend another interesting result of Aschner et al. [5] which ensures the connectivity of two sets of oriented four points that are separated by a straight line. Our extension (which is given in Theorem 3) relaxes the linear separability constraint. Most of the paper is devoted to proving this theorem.

1.2 Some related problems

There is a relationship between bounded-angle spanning trees and bounded-degree spanning trees which have received a considerable attention [7, 12, 17, 19, 20, 22]. A degree-k ST is a spanning tree in which every vertex has degree at most k. It is easily seen that any degree-k ST is an α-ST with $\alpha = 2\pi(1 - 1/k)$ because in any degree-k ST all edges that are incident to each vertex lie in some wedge of angle $2\pi(1 - 1/k)$.

The α-bottleneck spanning tree (α-BST) is a closely related problem in which the goal is to compute an α-ST whose longest edge length is minimum. This problem has been studied in the context of designing networks with bounded-range directional antennas, see for example the results of Aschner et al. [3, 5] for constructing hop-spanners for unit disk graphs, Dobrev et al. [14, 15] and Caragiannis et al. [10] for constructing bounded-degree strongly connected networks, and Carmi et al. [11] for constructing bounded-angle Hamiltonian paths. Another related problem in this context is "power assignment with directional antennas" where the objective is to assign each point $p \in P$ a wedge of angle α as well as a range r_p to obtain a connected symmetric communication network of minimum total power $\sum_{p\in P}(r_p)^\beta$ where $\beta \geqslant 1$ is the distance-power gradient [3, 5, 23].

Computing bounded-angle Hamiltonian paths and cycles on points in the plane is another related problem. For paths it is known that any set of points in the plane admits a Hamiltonian path with turning angles at most $\frac{\pi}{2}$ [11, 18] and this bound on the angle is tight [11, 16]. For cycles no tight bound on the angle is known. Dumitrescu et al. [16] proved that any even-size point set admits a Hamiltonian cycle with angles at most $\frac{2\pi}{3}$. The most famous conjecture in this context, due to Fekete and Woeginger [18], states that any even-size point set of at least 8 elements admits a Hamiltonian cycle with angles at most $\frac{\pi}{2}$.

1.3 Preliminaries for the algorithm

The following notations are adopted from [8]. Let w_p be a wedge in the plane having its apex at a point p. We denote the clockwise (right) boundary ray of w_p by $\overrightarrow{w_p}$ and its counterclockwise (left) boundary ray by $\overleftarrow{w_p}$. Let w_q be another wedge in the plane having its apex at a point q. If q lies in w_p then we say that p *sees* q (or q is *visible* from p). We say that p and q are *mutually visible*, denoted by $p \leftrightarrow q$, if p sees q and q sees p. In Figure 2 p and q are mutually visible. Let P be a set of points in the plane such that some wedge is placed at each point of P. The *induced mutual visibility graph* of P, denoted by $G(P)$, is a geometric graph with vertex set P that has a straight-line edge between two points $p, q \in P$ if and only if p and q are mutually visible. We use the term "orient" to refer to placement of wedges at points. We denote the sum of edge lengths of a geometric graph G by $w(G)$.

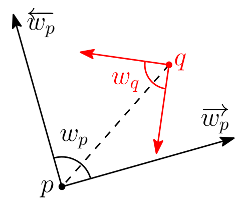

Figure 2 The points p and q are mutually visible.

We define the following notations to facilitate the description of our algorithm and its analysis. For two points p and q in the plane the *slab* $S(p, q)$ is defined as the region between two lines that are perpendicular to the segment pq at points p and q (see Figure 3(a)). We use *quadruple* to denote a set of four points in the plane. A quadruple Q is called *admissible* if it has two points p and q such that the other two points lie in $S(p, q)$ and both on the same side of pq. In this case we refer to (p, q) as an *admissible pair* of Q. Notice that a quadruple could have more than one admissible pair. For a quadruple Q with a fixed admissible pair (p, q), we define the *admissible slab* of Q, denoted by $S(Q)$, to be the same as the slab $S(p, q)$; see Figure 3(a). The following lemma (though very simple) plays an important role in our algorithm.

▶ **Lemma 1.** *Any set P of five points in the plane contains an admissible quadruple Q such that all points of P lie in $S(Q)$.*

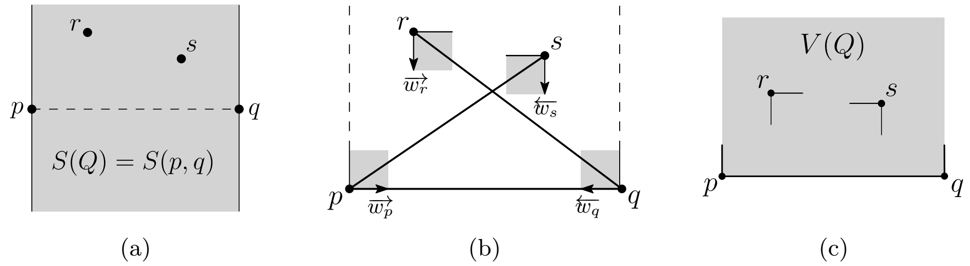

Figure 3 An admissible quadruple $Q = \{p, q, r, s\}$ with admissible pair (p, q). Illustrations of (a) the slab $S(p, q)$ which is the same as the admissible slab $S(Q)$, (b) the proof of Theorem 2, and (c) the visibility region $V(Q)$ which is the region visible to both p and q.

Proof. Let p and q be two points that define a diameter of P, i.e., two with maximum distance. Of the remaining three points of P at least two of them, say r and s, lie on the same side of $S(p, q)$. Therefore $\{p, q, r, s\}$ is an admissible quadruple which we denote by Q. Since pq is a diameter of P, all points of P lie in $S(p, q)$ and hence in $S(Q)$. ◀

Our orientation of admissible quadruples in the following theorem is similar to that of Aschner, Katz, and Morgenstern et al. [5] for arbitrary quadruples.

▶ **Theorem 2.** *Given an admissible quadruple Q, one can place at each point of Q a wedge of angle $\pi/2$ such that the wedges cover the plane and the induced mutual visibility graph of Q is connected.*

Proof. Let $Q = \{p, q, r, s\}$. After a suitable relabeling, rotation and reflection assume that (p, q) is an admissible pair of Q, the line segment pq is horizontal, p is to the left of q, the points r and s lie above pq, and r is to the left of s as in Figure 3(b). We place four wedges at points of Q as in Figure 3(b). Formally, we place a wedge w_p at p such that $\overrightarrow{w_p}$ passes through q, place w_q at q such that $\overleftarrow{w_q}$ passes through p, place w_r at r such that q lies in w_r and $\overrightarrow{w_r}$ is vertical, and place w_s at s such that p lies in w_s and $\overleftarrow{w_s}$ is vertical. These four wedges cover the entire plane (if we think of the intersection point of $\overrightarrow{w_p}$ and $\overrightarrow{w_r}$ as the origin of the coordinate system, then the four wedges cover the four quadrants). Moreover, the induced mutual visibility graph is connected because $p \leftrightarrow q$, $r \leftrightarrow q$, and $p \leftrightarrow s$. ◀

Recall the two points p and q in the proof of Theorem 2 that make Q admissible. Notice that after orientation of Theorem 2 the admissible slab of Q is uniquely defined by p and q. We define the *visibility region* of Q, denoted by $V(Q)$, as part of $S(Q)$ that is visible to both p and q; see Figure 3(c) for an illustration.

The following theorem, which will be proved in Section 3, plays a crucial role in the correctness of our algorithm. Most of the paper is devoted to proving this theorem.

▶ **Theorem 3.** *Let Q_1 and Q_2 be two admissible quadruples. Assume that wedges of angle $\pi/2$ are placed at points of each of Q_1 and Q_2 according to the placement in the proof of Theorem 2. Then at least one of the following statements holds*

(i) *The induced mutual-visibility graph of $Q_1 \cup Q_2$ is connected.*

(ii) *At any point p in $S(Q_1) \cup S(Q_2)$ one can place a wedge of angle $\pi/2$ such that p is mutually visible from a point $q_1 \in Q_1$ and from a point $q_2 \in Q_2$. In other words the induced mutual-visibility graph of $Q_1 \cup Q_2 \cup \{p\}$ is connected.*

We note that there are admissible quadruples for which statement (i) does not hold, but (ii) holds for them; see for example Figure 12. Theorem 3 extends the following result of Aschner et al. [5] which applies only to quadruples that are separated by a line.

▶ **Theorem 4** (Aschner, Katz, and Morgenstern [5], 2013). *Let Q_1 and Q_2 be two quadruples. Assume that wedges of angle $\pi/2$ are placed at points of each of Q_1 and Q_2 according to the placement in the proof of Theorem 2. If Q_1 and Q_2 are separated by a straight line, then the induced mutual-visibility graph of $Q_1 \cup Q_2$ is connected.*

2 The approximation algorithm

Let P be a set of n points in the plane. In this section we present our algorithm for computing a $\frac{\pi}{2}$-ST of P of weight at most 10 times the weight of the MST of P. In Section 2.1 we describe the general framework of the algorithm. In Section 2.2 we provide the details of the algorithm and its analysis.

2.1 A general framework

Our algorithm follows the same framework as previous algorithms [3, 6, 8] which is described below. This framework was first introduced by Aschner and Katz [3].

Start by computing an MST of P. From the MST obtain a Hamiltonian path H of weight at most 2 times the weight of MST. It is well-known that such a path can be obtained by doubling the MST edges, computing an Euler tour, and then short-cutting repeated vertices. The constant 2 is tight as Fekete et al. [17] showed that for any fixed $\varepsilon > 0$ there exist point sets for which the weight of any Hamiltonian path is at least $2 - \varepsilon$ times the weight of MST.

The next step is to partition H into $\frac{n}{k}$ groups each consisting of k consecutive vertices of H for some constant k (assuming n is divisible by k). Then orient each group independently in such a way that (I) the vertices in each group are connected, and (II) there is an edge between any pair of consecutive groups. Thus the induced mutual visibility graph on P is connected. Moreover, as the vertices of the groups are connected locally (to the vertices of the same group or a neighboring group), the mutual visibility graph contains a spanning tree whose weight is within some constant factor of the weight of H. This constant depends only on k.

The original algorithms of Aschner and Katz [3] partition H into groups of size $k = 8$ for $\alpha = \frac{\pi}{2}$ and $k = 3$ for $\alpha = \frac{2\pi}{3}$. The improved algorithms of [8] and [6] (for $\alpha = \frac{2\pi}{3}$) partition H into groups of size $k = 3$ and $k = 2$, respectively.

Our algorithm partitions H into groups of size $k = 5$ for $\alpha = \frac{\pi}{2}$. The most challenging part in our algorithm (and in previous algorithms) is to maintain property (II); the proof of this property often involves detailed case analysis. There is a main difference between our algorithm and previous algorithms [3, 6, 8]. Instead of orienting all five vertices in each group simultaneously, we first *select* four of them and orient only these selected vertices. The four selected vertices form an admissible quadruple. We refer to the non-selected vertex as a *backup*. We show that, except for one "special case", there is always a connection between two oriented admissible quadruples. For the special case we use the backup vertex to make the connection between two quadruples.

2.2 Details of our algorithm

In this section we provide details of our algorithm and its analysis. Recall that P is a set of n points in the plane, and that H is a Hamiltonian path on P such that

$$w(H) \leqslant 2w(\mathrm{MST}).$$

Let $h_1, \dots, h_{n-1}$ be the sequence of edges of H from one end to another. Partition the edges of H into five sets $H_1 = \{h_1, h_6, \dots\}$, $H_2 = \{h_2, h_7, \dots\}$, $H_3 = \{h_3, h_8, \dots\}$, $H_4 = \{h_4, h_9, \dots\}$, and $H_5 = \{h_5, h_{10}, \dots\}$. Let H_k with $k \in \{1, 2, 3, 4, 5\}$ be the edge set with the largest weight. Then

$$w(H_k) \geqslant \frac{w(H)}{5} \quad \text{and} \quad w(H \setminus H_k) \leqslant \frac{4w(H)}{5}.$$

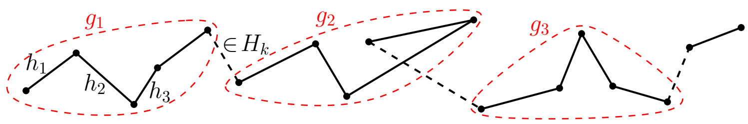

Figure 4 Illustration of the groups and sub-paths (dashed edges belong to H_k, where $k = 5$).

By removing all edges of H_k from H we obtain a sequence of sub-paths each containing five vertices (except possibly the first and last sub-paths). To simplify our description we assume for now that all sub-paths have five vertices, later in Remark 5 we will take care of the case where the first and last sub-paths have less than five vertices. We refer to the five vertices of each sub-path as a *group*. Let $g_1, g_2, \dots, g_m$ denote the sequence of the groups that is corresponding to the sequence of sub-paths along H as in Figure 4.

From each group g_i we take an admissible quadruple Q_i (consisting of four vertices) as in the proof of Lemma 1. We denote the remaining vertex of g_i by b_i; this is a backup vertex. By Lemma 1, b_i lies in $S(Q_i)$. We orient each admissible quadruple Q_i according to the orientation in the proof of Theorem 2 which ensures the connectivity of the induced mutual visibilty graph $G(Q_i)$. Consider any two consecutive oriented quadruples Q_i and Q_{i+1}. By Theorem 3 at least one of the following statements holds:

(i) The graph $G(Q_i \cup Q_{i+1})$ is connected, i.e., there is an edge between Q_i and Q_{i+1}.

(ii) Any point p in $S(Q_i) \cup S(Q_{i+1})$ can be oriented so that $G(Q_i \cup Q_{i+1} \cup \{p\})$ is connected.

If statement (i) holds then we orient b_i towards a vertex of Q_i that sees b_i (such a vertex exists because the orientation of Theorem 2 covers the entire plane). If (i) does not hold but (ii) holds then we orient b_i in such a way that it connects Q_i and Q_{i+1}.

To this end all vertices are oriented except the backup vertex b_m of g_m. We orient b_m towards a vertex of Q_m that sees b_m. Thus, we obtain a connected induced mutual visibility graph $G(P)$.

Now we obtain a spanning tree T of $G(P)$ as follows: First we take an arbitrary spanning tree T_i from each $G(Q_i)$. Then we connect each pair T_i and T_{i+1} either by a direct edge (if (i) holds) or via a backup vertex (if (ii) holds). Lastly we connect any remaining backup vertex to its corresponding quadruple by an edge. This gives a spanning tree T that we report as the output of our algorithm. Notice that the trees T_i are not necessarily minimum spanning trees of graphs $G(Q_i)$; we will use the triangle inequality to bound the length of T.

Analysis of the approximation ratio. To bound the weight of T, we charge the edges of H for the edges of T as follows. By the triangle inequality, the weight of every edge (p, q) of T is at most the weight of the unique path in H between p and q. We charge the weight of the edges of this path for the edge (p, q). Every edge of H_k is charged only once and that is for connecting two consecutive trees T_i and T_{i+1} (either directly or via a backup vertex). Every edge of $H \setminus H_k$ (i.e., every edge of each sub-path) is charged at most six times: three times for the three edges of T_i, two times for the two edges connecting T_i to T_{i+1} and to T_{i-1}, and once for the edge connecting the backup vertex b_i to T_i. Therefore

$$\begin{aligned} w(T) &\leqslant w(H_k) + 6w(H \setminus H_k) \\ &= w(H) + 5w(H \setminus H_k) \leqslant w(H) + 5 \cdot \frac{4w(H)}{5} = 5w(H) \leqslant 10w(\mathrm{MST}). \end{aligned}$$

Running-time analysis. After computing an MST in $O(n \log n)$ time, the rest of the algorithm (computing H, finding H_k, orienting admissible quadruples and backup vertices, and obtaining T) takes $O(n)$ time.

▶ Remark 5. Here we handle the case where the first sub-path, denoted by δ, has less than five vertices (the last sub-path will be treated analogously). This case is essentially a simple version of Theorem 3 where fewer points are involved. We will use Theorem 3 to handle this case, however it could also be handled directly but with some case analysis.

We will connect the vertices of δ to g_1 (the first 5-vertex group). Let Q be g_1's admissible quadruple. Since the oriented points in Q cover the entire plane, it might be tempting to orient each point p of δ towards the point of Q that sees p. This approach may not be suitable when δ has more than one point because to maintain the ratio 10 we should not connect Q to its proceeding group (here to δ) by more than one edge. To remedy this, we use our Theorem 3.

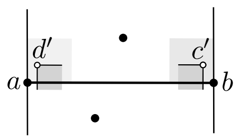

Figure 5 ab is the diameter of δ, and c', d' are fake points.

As discussed above, we may assume that δ has 2, 3, or 4 points. Let ab be a diameter of δ as in Figure 5. Thus, δ has points a, b, and at most two other "real" points. We place a "fake" point c' in $S(a, b)$ and very close to b such that both c' and b lie on the same side of any line through boundary rays of wedges in Q. In the same fashion we place a fake point d' very close to a, and on the same side of ab as c'. Let $Q' = \{a, b, c', d'\}$. Our placement of c' and d' – in $S(a, b)$ and on the same side of ab – implies that Q' is an admissible quadruple with admissible pair (a, b). We orient Q' according to Theorem 2. By Theorem 3-part (i), a point of Q' and a point of Q are mutually visible (our placement of c' and d' together with Property 1 from the next section imply that part (i) of Theorem 3 holds). If the visibility is through a real point say b, then we reflect the orientation of a with respect to ab. After reflection, a and b remain mutually visible, and their wedges cover the entire region $S(a, b)$. Then we orient every other real vertex of δ towards the one of a and b that sees it. If the visibility is through a fake point say c' then the point of Q, say q, that sees c' also sees b (this is implied by our placement of c'). In this case we reflect the orientation of b with respect to ab so that b is mutually visible with q, and a and b together see the entire region $S(a, b)$.

Then we orient every other real vertex of δ towards the one of a and b that sees it. In either case we remove fake points. Therefore the mutual visibility graph on points of δ is connected, and it has a connection to a point in Q via a or b.

The following theorem summarizes our main result.

▶ **Theorem 6.** *For any set of points in the plane and any angle $\alpha \geqslant \frac{\pi}{2}$, there is an α-spanning tree of length at most 10 times the length of the MST. Furthermore, there is an algorithm that finds such an α-spanning tree in linear time after construction of the MST.*

3 Proof of Theorem 3

In this section we prove Theorem 3 which says: *Let Q_1 and Q_2 be two admissible quadruples. Assume that wedges of angle $\pi/2$ are placed at points of each of Q_1 and Q_2 according to the placement in the proof of Theorem 2. Then at least one of the following statements holds*

(i) *The induced mutual-visibility graph of $Q_1 \cup Q_2$ is connected.*

(ii) *At any point p in $S(Q_1) \cup S(Q_2)$ we can place a wedge of angle $\pi/2$ such that p is mutually visible from a point $q_1 \in Q_1$ and from a point $q_2 \in Q_2$. In other words the induced mutual-visibility graph of $Q_1 \cup Q_2 \cup \{p\}$ is connected.*

Our proof is involved. For a better understanding we split our proof into smaller pieces based on the relative position of admissible pairs of Q_1 and Q_2. Let $Q_1 = \{a, b, c, d\}$ and $Q_2 = \{a', b', c', d'\}$. After a suitable relabeling assume that (a, b) and (a', b') are the admissible pairs of Q_1 and Q_2, respectively, that are considered in the orientation of Theorem 2. Also assume that – after the orientation of Theorem 2 – c looks towards a while d looks towards b, and similarly c' looks towards a' while d' looks towards b' as in Figures 7-13. We use this notation throughout our proof without further mentioning. Up to symmetry we have the following four cases:

A. $a'b'$ intersects ab.

B. The extension of $a'b'$ intersects the extension of ab.

C. The extension of $a'b'$ intersects ab.

D. $a'b'$ is parallel to ab.

After a suitable rotation we assume that ab is horizontal and a is to the left of b. We denote by ℓ the line through ab and by ℓ' the line through $a'b'$ as in Figure 7(a). For a point x we denote by ℓ_x the line through x that is perpendicular to ℓ, and denote by ℓ'_x the line through x that is perpendicular to ℓ. For a line l in the plane we use the terms "above" and "below" to refer to the two half planes on the two sides of l. If l is vertical then "below" refers to the left-side half plane and "above" refers to the right-side half plane. Throughout our proof, we use the following obvious observation about mutual visibility without mentioning it in all occurrences.

▶ **Observation 7.** *Assume that wedges w_p and w_q of angles $\frac{\pi}{2}$ are placed at two points p and q. If the clockwise (resp. counterclockwise) boundary ray of w_p meets the counterclockwise (resp. clockwise) boundary ray of w_q at an obtuse or a right angle then p and q are mutually visible. See Figure 6.*

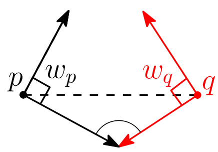

Figure 6 Illustration of Observation 7.

Some part of our proof (where Q_1 and Q_2 are separated by a line) could be implied from Theorem 4. However, for the sake of completeness we provide our own proof. We provide the proof of the first cases, A and B-1, with more formal details. To simplify our description, we will refer to the clockwise (resp. counterclockwise) boundary ray of the wedge that is placed at a point p by "the clockwise (resp. counterclockwise) ray of p".

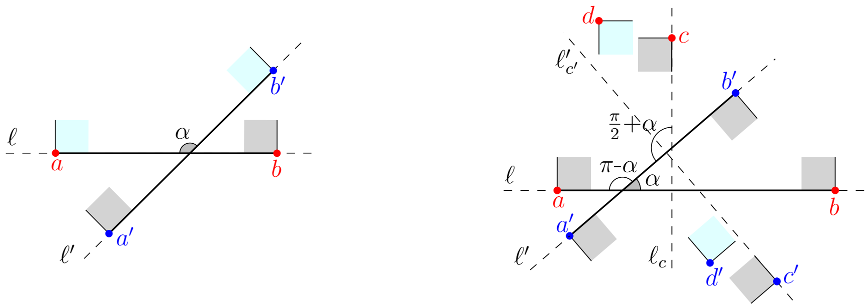

(a) A-1

(b) A-2: c' below ℓ, c above ℓ'

Figure 7 Illustration of the proof of case A.

A. $a'b'$ intersects ab

We denote by α the intersection angle of ab and $a'b'$ that lies in $V(Q_1) \cap V(Q_2)$. We say that α is *defined* by the two vertices that lie on this angle. For example in Figure 7(a) the angle α is defined by a and b'. Depending on the value of α we consider the following two cases.

1. $\alpha \geqslant \frac{\pi}{2}$. After a suitable relabeling we assume that α is defined by a and b', as in Figure 7(a). In this case the clockwise ray of a and the counterclockwise ray of b' meet at angle α, and thus a and b' are mutually visible by Observation 7.
2. $\alpha < \frac{\pi}{2}$. After a suitable relabeling we assume that α is defined by b and b', as in Figure 7(b). If c' is above ℓ then the clockwise ray of a and the counterclockwise ray of c' meet at angle $\pi - \alpha$, and thus c' and a are mutually visible by Observation 7. Similarly if c is below ℓ' then c and a' are mutually visible. Assume that c' is below ℓ and c is above ℓ' as in Figure 7(b). If d' is to the left of ℓ_c then the clockwise ray of d' and the counterclockwise ray of c meet at angle $\frac{\pi}{2} + \alpha$, and thus d' and c are mutually visible by Observation 7. Similarly if d is below $\ell'_{c'}$ then d and c' are mutually visible. Assume that d' is to the right of ℓ_c, and d is above $\ell'_{c'}$. In this setting which is depicted in Figure 7(b), d and d' lie in opposite cones formed by intersection of ℓ_c and $\ell'_{c'}$, and thus d and d' are mutually visible (observe that the clockwise ray of d and the counterclockwise ray of d' meet at angle $\pi - \alpha$).

B. The extension of $a'b'$ intersects the extension of ab

Let α be the angle at which the extensions of ab and $a'b'$ meet each other as in Figures 8 and 9. After a suitable reflection and relabeling we assume that $a'b'$ lies below ℓ, their extensions meet at a point m to the right of b, and a' is farther from m than b'. Depending on the value of α we consider two cases.

1. $\alpha \geqslant \frac{\pi}{2}$. Depending on visibility regions of Q_1 and Q_2 we consider three sub-cases (up to symmetry).
    1. $V(Q_1)$ lies below ab and $V(Q_2)$ lies below $a'b'$ as in Figure 8(a). In this case the clockwise ray of a' and the counterclockwise ray of a meet at angle α, and hence $a \leftrightarrow a'$ by Observation 7.

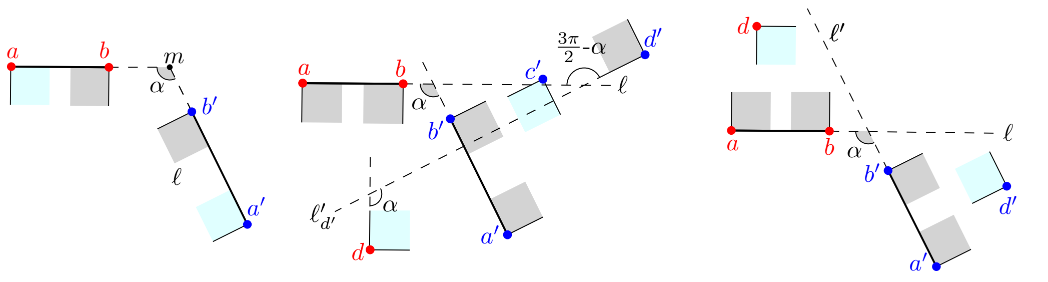

(a) B-1-1 (b) B-1-2: d' above ℓ, d below $\ell'_{d'}$ (c) B-1-3: d' below ℓ, d below ℓ'

Figure 8 Illustration of the proof of case B-1.

2. $V(Q_1)$ lies below ab and $V(Q_2)$ lies above $a'b'$. See Figure 8(b). If d' is below ℓ then the clockwise ray of d' and the counterclockwise ray of a meet at angle α and hence $a \leftrightarrow d'$. Assume that d' is above ℓ. If d is above $\ell'_{d'}$ then the clockwise ray of d and the counterclockwise ray of d' meet at angle $\frac{3\pi}{2} - \alpha$ and thus $d \leftrightarrow d'$. Assume that d is below $\ell'_{d'}$. In this setting which is depicted in Figure 8(b) the clockwise ray of c' and the counterclockwise ray of d meet at angle α and thus $c' \leftrightarrow d$.
3. $V(Q_1)$ lies above ab and $V(Q_2)$ lies above $a'b'$. See Figure 8(c). If d' is above ℓ then $a \leftrightarrow d'$. Similarly if d is above ℓ' then $a' \leftrightarrow d$. Assume that d' is below ℓ and d is below ℓ'. In this setting which is depicted in Figure 8(c) the clockwise ray of d' and the counterclockwise ray of d meet at angle α and thus $d \leftrightarrow d'$.

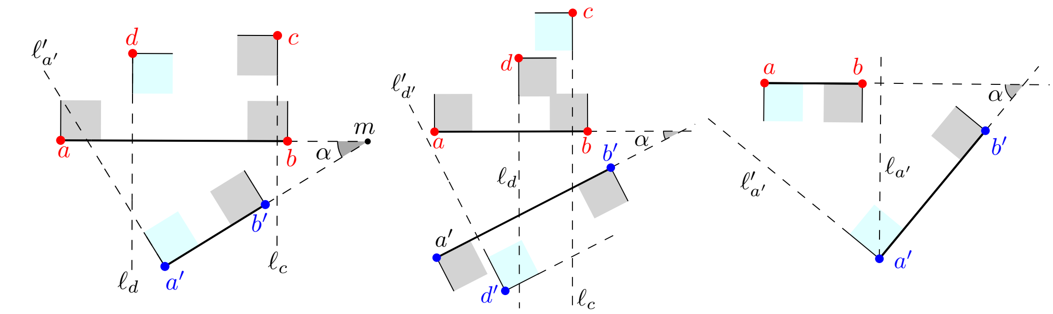

(a) B-2-1: d above $\ell'_{a'}$, a' right of ℓ_d (b) B-2-2: d' left of ℓ_d (c) B-2-3: b left of $\ell_{a'}$

Figure 9 Illustration of the proof of case B-2.

2. $\alpha < \frac{\pi}{2}$. Similar to the previous case here we also consider three sub-cases.
   1. $V(Q_1)$ lies above ab and $V(Q_2)$ lies above $a'b'$. See Figure 9(a). If d is below $\ell'_{a'}$ then d and b' are mutually visible. If a' is to the left of ℓ_d then a' and c are mutually visible. Assume that d is above $\ell'_{a'}$ and a' is to the right of ℓ_d as in Figure 9(a). In this setting d and a' are mutually visible.
   2. $V(Q_1)$ lies above ab and $V(Q_2)$ lies below $a'b'$. If d' is to the left of ℓ_d then $c \leftrightarrow d'$ as in Figure 9(b). Analogously if d is below $\ell'_{d'}$ then $c' \leftrightarrow d$. Therefore assume that d' is to right of ℓ_d and d is above $\ell'_{d'}$. In this setting $d \leftrightarrow d'$.
   3. $V(Q_1)$ lies below ab and $V(Q_2)$ lies above $a'b'$. See Figure 9(c). Consider $\ell_{a'}$, i.e., the line through a' that is perpendicular to ℓ. If b is to the right of $\ell_{a'}$ then $a' \leftrightarrow b$. Assume that b is to the left of $\ell_{a'}$ as in Figure 9(c). Now we look at $\ell'_{a'}$. If a is above this line then $a \leftrightarrow a'$, otherwise $a \leftrightarrow b'$. (Notice that when a is above $\ell'_{a'}$ then a and b' may not be mutually visible, for example when b' is very close to a'.)

C. The extension of $a'b'$ intersects ab

We denote by m the intersection point of ℓ' and ab. After a suitable reflection and relabeling we assume that $a'b'$ lies below ℓ, a' is farther from m than b', and angle $\angle a'ma \leqslant \frac{\pi}{2}$, as in Figure 10. Depending on visibility regions of Q_1 and Q_2 we consider four cases.

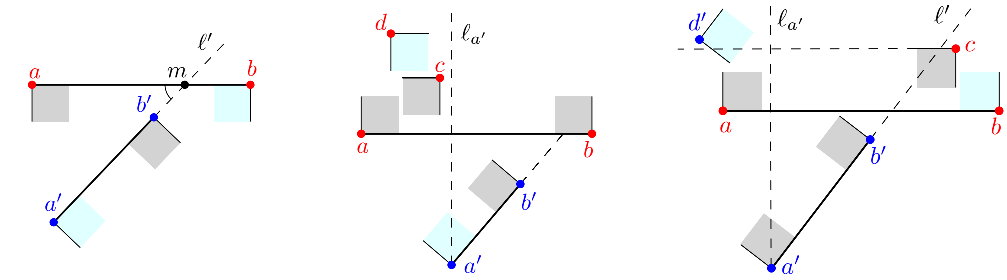

(a) C-1 (b) C-2: c left of $\ell_{a'}$ (c) C-2: c below ℓ'

Figure 10 Illustration of the proof of cases C-1 and C-2.

1. $V(Q_1)$ lies below ab and $V(Q_2)$ lies below $a'b'$ as in Figure 10(a). In this case $a' \leftrightarrow b$.
2. $V(Q_1)$ lies above ab and $V(Q_2)$ lies above $a'b'$. If c is to the left of $\ell_{a'}$ then so is d, as in Figure 10(b). In this case d sees both a' and b', and at least one of a' and b' sees d, and thus $d \leftrightarrow a'$ or $d \leftrightarrow b'$. Assume that c is to the right of $\ell_{a'}$. If c is above ℓ' then $c \leftrightarrow a'$. Thus, assume that c is below ℓ' as in Figure 10(c). Recall that d' is in slab $S(a', b')$. If d' is above the horizontal line through c then $d' \leftrightarrow b$, otherwise $d' \leftrightarrow c$.

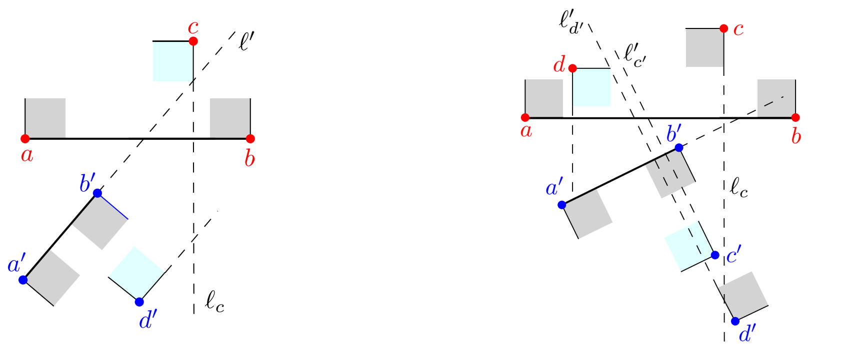

(a) C-3: d' left of ℓ_c (b) C-3: d' right of ℓ_c, d below $\ell'_{d'}$

Figure 11 Illustration of the proof of case C-3.

3. $V(Q_1)$ lies above ab and $V(Q_2)$ lies below $a'b'$. This case is depicted in Figure 11. If c is below ℓ' then $c \leftrightarrow a'$. Assume that c is above ℓ'. If d' is to the left of ℓ_c then $c \leftrightarrow d'$ as in Figure 11(a). Assume that d' is to the right of ℓ_c (and hence to the right of ℓ_d). Now we look at d with respect to $\ell'_{d'}$. If d is above $\ell'_{d'}$ then $d \leftrightarrow d'$. If d is below $\ell'_{d'}$ then it is also below $\ell'_{c'}$ and thus $d \leftrightarrow c'$ as in Figure 11(b).
4. $V(Q_1)$ lies below ab and $V(Q_2)$ lies above $a'b'$. This case is depicted in Figure 12. If d' is below ℓ then $d' \leftrightarrow b$. Assume that d' is above ℓ. If a is below $\ell'_{b'}$ then $a \leftrightarrow b'$. Assume that a is above $\ell'_{b'}$. If c is above $\ell'_{d'}$ then $c \leftrightarrow d'$. Assume that c is below $\ell'_{d'}$ (which is also below $\ell'_{c'}$). Notice that c' lies in the slab bounded by $\ell'_{b'}$ and $\ell'_{d'}$. If c' is to the left

of ℓ_c then $c' \leftrightarrow c$. Assume that c' is to the right of ℓ_c. Notice that d lies in the vertical slab bounded by ℓ_a and ℓ_c. Let ℓ_1 be the line through c' parallel to ℓ'. If d is below ℓ_1 then $d \leftrightarrow c'$. Assume that d is above ℓ_1. This configuration is depicted in Figure 12 (the caption of this figure summarizes the constraints). This is the configuration for which statement (i) of the theorem does not hold; for all other configurations statement (i) holds. We will show that statement (ii) holds in the current setting.

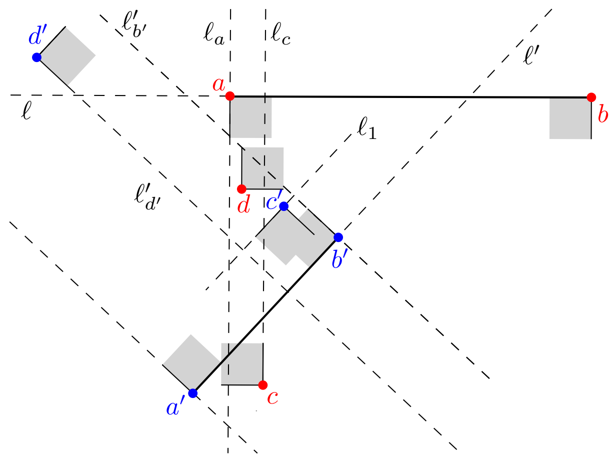

Figure 12 Illustration of case C-4: d' is above ℓ, a is above $\ell'_{b'}$, c is below $\ell'_{d'}$, c' is to the right of ℓ_c (and in the slab defined by $\ell'_{d'}$ and $\ell'_{b'}$), and d is above ℓ_1 (and in the slab defined by ℓ_a and ℓ_c). In this figure, Q_1 and Q_2 are oriented according to Theorem 2 but there is no mutual visibility between points of Q_1 and points of Q_2 (statement (i) in Theorem 3 does not hold here).

First, we extract a property of the current setting which is used in Remark 5. See Figure 12 for a better understanding of this property, and notice that in the current setting the points b, c lie on different sides of $\ell'_{b'}$, and the points a', d' lie on different sides of ℓ.

▶ **Property 1.** *If statement* (i) *in Theorem 3 does not hold then then the points b, c or the points a, d of Q_1 lie on different sides of a line through boundary rays of wedges of Q_2, and similarly the points b', c' or the points a', d' of Q_2 lie on different sides of a line through boundary rays of wedges of Q_1.*

To verify that statement (ii) holds in the current setting, let p be any point in the region $S(Q_1) \cup S(Q_2)$. We show how to place a wedge of angle $\frac{\pi}{2}$ at p so that p is mutually visible from a point in Q_1 and a point in Q_2. To simplify our description we partition $S(Q_1) \cup S(Q_2)$ into eight regions $R_1, \ldots, R_8$ as in Figure 13. If $p \in R_1$ then we orient p similar to d', and thus $p \leftrightarrow b$ and $p \leftrightarrow b'$. If $p \in R_2$ then we orient p similar to a, and thus $p \leftrightarrow c$ and $p \leftrightarrow b'$. If $p \in R_3$ then we orient it similar to c' so that $p \leftrightarrow c$ and $p \leftrightarrow a'$. If $p \in R_4$ then we orient it similar to b so that $p \leftrightarrow d$ and $p \leftrightarrow a'$. If $p \in R_5$ then we orient it similar to b', and hence $p \leftrightarrow d$ and $p \leftrightarrow d'$. If $p \in R_6$ then we orient it similar to c, and thus $p \leftrightarrow a$ and $p \leftrightarrow d'$. If $p \in R_7$ then we orient it similar to a' so that $p \leftrightarrow a$ and $p \leftrightarrow c'$. Finally if $p \in R_8$ then we orient it similar to d, and hence $p \leftrightarrow b$ and $p \leftrightarrow c'$. Thus statement (ii) of the theorem holds.

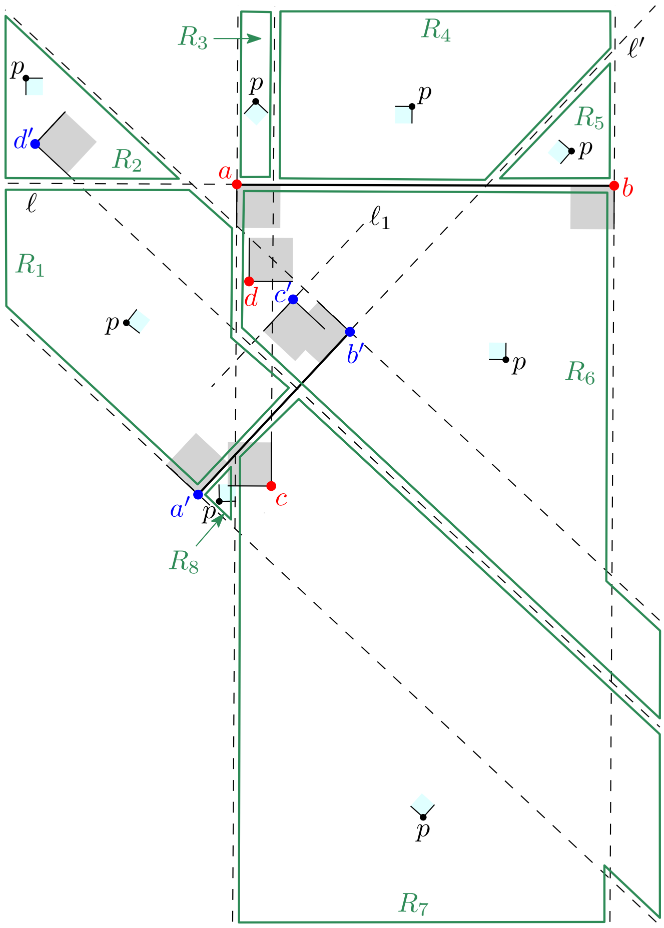

Figure 13 Partitioning $S(Q_1) \cup S(Q_2)$ into regions $R_1, \dots, R_8$.

D. $a'b'$ is parallel to ab

Assume that ab and $a'b'$ are horizontal, and ab lies above $a'b'$. Consider any horizontal line h between ab and $a'b'$. One pair of points from Q_1 (either (a, b) or (c, d)) covers the half plane below h. Also, one pair of points from Q_2 (either (a', b') or (c', d')) covers the half plane above h. One can simply verify that there is an edge between these two pairs in the induced mutual visibility graph.

This is the end of our proof of Theorem 3.

4 Conclusions

The obvious open problem is to improve our approximation ratio 10 which we think is not the best possible ratio. The use of a Hamiltonian path is a bottleneck towards our analysis as it forces a factor of 2 in the ratio. It might be possible to get better ratios by using the original MST instead of the path. Perhaps the MST may not be the best lower bound either because one may obtain a better ratio by considering the $\frac{\pi}{2}$-MST as a lower bound.

References

1 Eyal Ackerman, Tsachik Gelander, and Rom Pinchasi. Ice-creams and wedge graphs. *Computational Geometry: Theory and Applications*, 46(3):213–218, 2013.

2 Oswin Aichholzer, Thomas Hackl, Michael Hoffmann, Clemens Huemer, Attila Pór, Francisco Santos, Bettina Speckmann, and Birgit Vogtenhuber. Maximizing maximal angles for plane straight-line graphs. *Computational Geometry: Theory and Applications*, 46(1):17–28, 2013. Also in *WADS'07*.

3 Rom Aschner and Matthew J. Katz. Bounded-angle spanning tree: Modeling networks with angular constraints. *Algorithmica*, 77(2):349–373, 2017. Also in *ICALP'14*.

4 Rom Aschner, Matthew J. Katz, and Gila Morgenstern. Do directional antennas facilitate in reducing interferences? In *Proceedings of the 13th Scandinavian Symposium and Workshops on Algorithm Theory* (*SWAT*), pages 201–212, 2012.

5 Rom Aschner, Matthew J. Katz, and Gila Morgenstern. Symmetric connectivity with directional antennas. *Computational Geometry: Theory and Applications*, 46(9):1017–1026, 2013. Also in *ALGOSENSORS'12*.

6 Stav Ashur and Matthew J. Katz. A 4-approximation of the $\frac{2\pi}{3}$-MST. In *Proceedings of the 17th Algorithms and Data Structures Symposium (WADS)*, 2021.

7 Ahmad Biniaz. Euclidean bottleneck bounded-degree spanning tree ratios. *Discrete & Computational Geometry*, https://doi.org/10.1007/s00454-021-00286-4, 2021. Also in *SODA'20*.

8 Ahmad Biniaz, Prosenjit Bose, Anna Lubiw, and Anil Maheshwari. Bounded-Angle Minimum Spanning Trees. In *Proceedings of the 17th Scandinavian Symposium and Workshops on Algorithm Theory (SWAT 2020)*, pages 14:1–14:22, 2020.

9 Prosenjit Bose, Paz Carmi, Mirela Damian, Robin Y. Flatland, Matthew J. Katz, and Anil Maheshwari. Switching to directional antennas with constant increase in radius and hop distance. *Algorithmica*, 69(2):397–409, 2014. Also in *WADS'11*.

10 Ioannis Caragiannis, Christos Kaklamanis, Evangelos Kranakis, Danny Krizanc, and Andreas Wiese. Communication in wireless networks with directional antennas. In *Proceedings of the 20th Annual ACM Symposium on Parallelism in Algorithms and Architectures* (*SPAA*), pages 344–351, 2008.

11 Paz Carmi, Matthew J. Katz, Zvi Lotker, and Adi Rosén. Connectivity guarantees for wireless networks with directional antennas. *Computational Geometry: Theory and Applications*, 44(9):477–485, 2011.

12 Timothy M. Chan. Euclidean bounded-degree spanning tree ratios. *Discrete & Computational Geometry*, 32(2):177–194, 2004. Also in *SoCG'03*.

13 Mirela Damian and Robin Y. Flatland. Spanning properties of graphs induced by directional antennas. *Discrete Mathematics, Algorithms and Applications*, 5(3), 2013.

14 Stefan Dobrev, Evangelos Kranakis, Danny Krizanc, Jaroslav Opatrny, Oscar Morales Ponce, and Ladislav Stacho. Strong connectivity in sensor networks with given number of directional antennae of bounded angle. *Discrete Mathematics, Algorithms and Applications*, 4(3), 2012. Also in *COCOA'10*.

15 Stefan Dobrev, Evangelos Kranakis, Oscar Morales Ponce, and Milan Plzík. Robust sensor range for constructing strongly connected spanning digraphs in UDGs. In *Proceedings of the 7th International Computer Science Symposium in Russia* (*CSR*), pages 112–124, 2012.

16 Adrian Dumitrescu, János Pach, and Géza Tóth. Drawing Hamiltonian cycles with no large angles. *Electronic Journal of Combinatorics*, 19(2):P31, 2012. Also in *GD'94*.

17 Sándor P. Fekete, Samir Khuller, Monika Klemmstein, Balaji Raghavachari, and Neal E. Young. A network-flow technique for finding low-weight bounded-degree spanning trees. *Journal of Algorithms*, 24(2):310–324, 1997. Also in *IPCO* 1996.

18 Sándor P. Fekete and Gerhard J. Woeginger. Angle-restricted tours in the plane. *Computational Geometry: Theory and Applications*, 8:195–218, 1997.

19 Raja Jothi and Balaji Raghavachari. Degree-bounded minimum spanning trees. *Discrete Applied Mathematics*, 157(5):960–970, 2009.

20 Samir Khuller, Balaji Raghavachari, and Neal E. Young. Low-degree spanning trees of small weight. *SIAM Journal on Computing*, 25(2):355–368, 1996. Also in *STOC'94*.

21 Evangelos Kranakis, Fraser MacQuarrie, and Oscar Morales Ponce. Connectivity and stretch factor trade-offs in wireless sensor networks with directional antennae. *Theoretical Computer Science*, 590:55–72, 2015.

22 Clyde L. Monma and Subhash Suri. Transitions in geometric minimum spanning trees. *Discrete & Computational Geometry*, 8:265–293, 1992. Also in *SoCG'91*.

23 Tien Tran, Min Kyung An, and Dung T. Huynh. Antenna orientation and range assignment algorithms in directional WSNs. *IEEE/ACM Transaction on Networking*, 25(6):3368–3381, 2017. Also in *INFOCOM'16*.